ELSEVIER

Polymer Vol. 37 No. 6, pp. 925–929, 1996

0032-3861/96/$15.00+0.00

The protonation–deprotonation hysteresis in polyaniline

E. T. Kang* and K. G. Neoh
Department of Chemical Engineering, National University of Singapore, Kent Ridge, Singapore 119260

and K. L. Tan
Department of Physics, National University of Singapore, Kent Ridge, Singapore 119260
(Received 4 November 1994; revised 26 June 1995)

The changes in intrinsic oxidation state ([=N–] and [–NH–] content) and protonation level ([N^+]/[N] ratio) of emeraldine (EM) base powders as a function of protonic acid loadings resulting from the protonation–deprotonation cycle have been assessed quantitatively by X-ray photoelectron spectroscopy. A hysteresis effect was observed for the protonation–deprotonation cycle involving HCl, but not for H_2SO_4. The hysteresis has been attributed in part to covalent HCl addition to the polymer and the associated reduction in intrinsic oxidation state. A hysteresis effect involving a significant increase in intrinsic oxidation state was observed in the once acid–base cycled EM films cast from *N*-methylpyrrolidinone, but not for powders. The phenomenon has been attributed to the more efficient hydrolysis of powder samples in aqueous acid media due to the large effective surface area.

(Keywords: hysteresis; protonation–deprotonation; polyaniline)

INTRODUCTION

Recent investigations[1,2] into the century-old[3,4] aniline family of polymers have rekindled intense research intere in these materials. The aniline polymers generally have ontrollable electrical conductivity[1,2,5], environmental stability, solution-induced[7,8] and counterion-induced[9,10] processability, and interesting redox properties associated with the chain nitrogens[11,12]. More recent improvements in chemical processing have resulted in high-quality conducting polyaniline (PAN) with increased conductivity and crystallinity[13]. The aniline polymers have the general formula $[(-B-NH-B-NH-)_y(-B-N=Q=N-)_{1-y}]_x$, in which B and Q denote the C_6H_4 rings in the benzenoid and quinonoid forms, respectively. Thus, the aniline polymers are basically poly(*p*-phenylene amine imine)s, in which the intrinsic oxidation states can range from that of the fully reduced leucoemeraldine (LM, $y = 1$), through that of the 50% oxidized emeraldine (EM, $y = 0.5$), to that of the fully oxidized pernigraniline (PNA, $y = 0$). The polymer can achieve its highly conductive state either through the protonation of the imine nitrogens (=N–) in its EM oxidation state, or through the oxidation of the amine nitrogens (–NH–) in its fully reduced LM state[1,2]. Recent studies[12,14] have also shown that the amine nitrogens of the EM and LM oxidation states are also susceptible to protonation by strong, non-volatile acid. On the other hand, however, protonation of the 75% oxidized nigraniline (NA) base or the fully oxidized PNA base by an aqueous acid gives rise to only a 50% protonated EM base[12]. In view of the great importance of protonic acids on the electrical properties, the intrinsic oxidation states and the physical processability of PAN, it may be appropriate to revisit the protonation of EM base by two of the most commonly used protonic acids, viz. HCl and H_2SO_4. This effort is further spurred by the observed hysteresis in the conductivity of the polymer[5] as a function of the HCl protonic concentration during the protonation–deprotonation cycle.

EXPERIMENTAL

The emeraldine (EM)–HCl salt was prepared via the oxidative polymerization of aniline by ammonium persulfate in aqueous 1 M HCl, according to the procedures reported in the literature[2]. The EM–sulfate salt was prepared by the same method, but using 1 M H_2SO_4 as the polymerization medium instead. The EM salts were deprotonated to various extents by equilibrating the salt powders in dilute NaOH solutions of different pH values. Some of the EM salts were converted to the base polymer by treatment with an excess amount of 0.5 M NaOH. The EM base powders so obtained were subsequently reprotonated to various extents by equilibrating them in aqueous HCl or H_2SO_4 solutions of different pH values. The base polymer was also cast into thin films of about 5–8 μm thickness from *N*-methylpyrrolidinone (NMP) solution.

The intrinsic structures, in particular the intrinsic oxidation state (imine/amine ratios), and the protonation levels of the polymer films were determined by X-ray photoelectron spectroscopy (X.p.s.). The X.p.s.

* To whom correspondence should be addressed

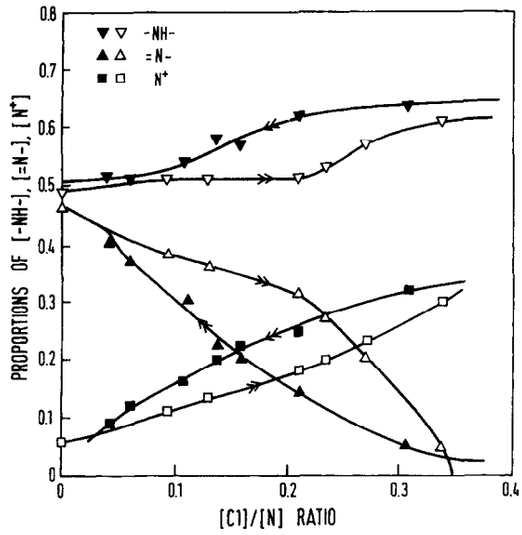

Figure 1 Changes in the intrinsic oxidation states and protonation levels of EM base powders during the protonation–deprotonation cycle involving HCl: closed symbols, deprotonation; open symbols, protonation

measurements were made on a VG Escalab Mk II spectrometer with a Mg Kα X-ray source (1253.6 eV photons) at a constant retard ratio of 40. The polymer powders were mounted on standard sample studs by means of double-sided adhesive tape. The X-ray source was run at a reduced power of 120 W (12 kV and 10 mA). To compensate for surface charging effects, all binding energies were referenced to the C 1s neutral carbon peak at 284.6 eV. All core-level spectra were obtained at a photoelectron take-off angle (with respect to the sample surface) of 75°. In peak synthesis, the linewidth (full width at half-maximum, FWHM) of the Gaussian peaks was maintained constant for all components in a particular spectrum. The elemental stoichiometries were determined from peak area ratios, after correcting with the experimentally determined sensitivity factors and were accurate to within ±10%.

RESULTS AND DISCUSSION

X.p.s. has been shown to be an ideal tool for the study of the intrinsic structure and charge transfer interactions in N-containing electroactive polymers[15]. In the case of polyaniline (PAN), the quinonoid imine (=N–), benzenoid amine (–NH–) and positively charged nitrogens corresponding to any particular intrinsic redox state and protonation level can be quantitatively differentiated in the properly curve-fitted N 1s core-level spectrum. They correspond to peak components with binding energies (BE) at about 398.2 eV, 399.4 eV and >400 eV, respectively.

Figure 1 summarizes the changes in intrinsic oxidation states (imine and amine contents) and protonation levels [N^+]/[N] mole ratios) with protonic acid loadings ([Cl]/[N] mole ratios), as revealed by X.p.s. analyses, during a typical protonation–deprotonation cycle of PAN involving HCl. The [Cl]/[N] ratios were determined from the sensitivity-factors-corrected Cl 2p and N 1s core-level spectra area ratios. Depending on whether the polymer is undergoing protonation or deprotonation, the intrinsic oxidation states and protonation levels of the polymer can vary substantially at a particular [Cl]/[N] ratio. Thus, a hysteresis effect in both the intrinsic oxidation states and protonation levels was observed in the protonation–deprotonation cycle.

In the wide-scan X.p.s. analyses of the EM–HCl and EM–H_2SO_4 complexes, only elements arising from the polymer (C and N) and the doping acids (Cl or S and O) were observed. *Figures 2a* and *2b* show, respectively, the

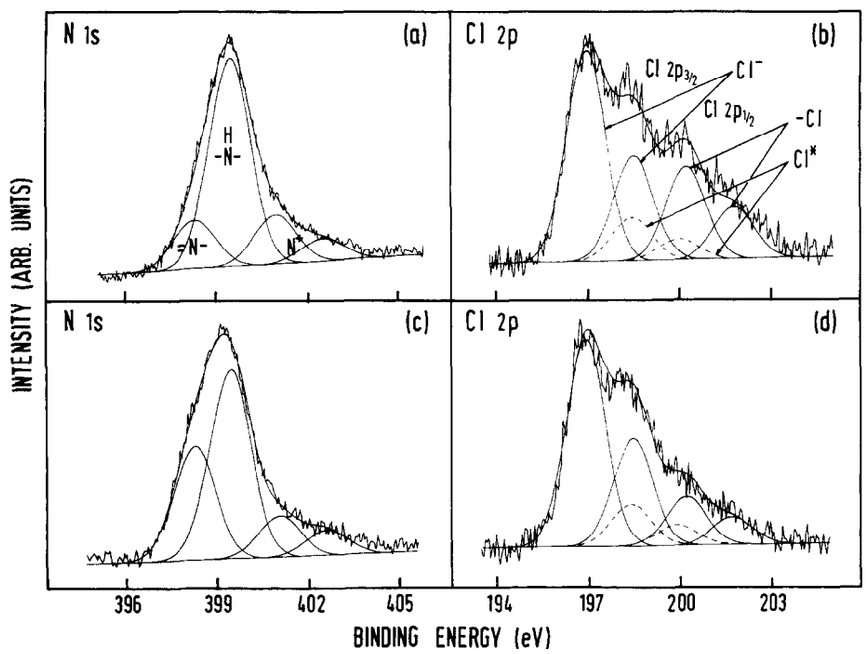

Figure 2 N 1s and Cl 2p core-level spectra for (a) and (b) a partially deprotonated EM–HCl powder ([Cl]/[N] = 0.21), and (c) and (d) a partially HCl-protonated EM powder ([Cl]/[N] = 0.21)

N 1s and Cl 2p core-level spectra for an EM–HCl salt after it had been subjected to partial deprotonation. The sample has a [Cl]/[N] ratio of about 0.21. The corresponding spectra for a sample with similar [Cl]/[N] ratio, but obtained via partial protonation of an EM base, are shown in *Figures 2c* and *2d*. Based on the fixed FWHM approach in peak synthesis used in the present work, the high BE tail in the N 1s spectrum, attributable to the protonated (positively charged) nitrogens, has been resolved into two peaks separated by about 1.5 eV and 3.0 eV from the amine peak, respectively. Nevertheless, the high BE tail is more appropriately ascribed to positively charged nitrogens with a continuous distribution of BEs, or positively charged nitrogens in a large number of different environments arising from inter- and intra-chain charge distributions. The Cl 2p core-level spectrum in each case is best resolved into three spin–orbit split doublets ($Cl\,2p_{3/2}$ and $Cl\,2p_{1/2}$), with the BEs for the $Cl\,2p_{3/2}$ peaks lying at about 197.1, 198.6 and 200.4 eV and a $Cl\,2p_{2/3}$ and $Cl\,2p_{1/2}$ component area ratio of 2 to 1. The high and low BE components suggest the presence of ionic (Cl^-) and covalent (–Cl) chlorine species, respectively[16]. The chlorine species with intermediate BE (Cl*, dashed component in the Cl 2p spectra), which has been widely observed[15,17,18], is more appropriately associated with anionic chloride species resulting from the charge transfer interactions between the halogen and the metal-like conducting state of the polymer chain. A fairly close balance between the amount of chloride anions (sum of Cl^- and Cl* species) and the proportion of the positively charged nitrogens was observed during the protonation cycle. For example, at a [Cl]/[N] ratio of 0.34 in *Figure 1*, a $[Cl^- + Cl^*]/[N]$ ratio of 0.29 and a $[N^+]/[N]$ ratio of 0.30 was observed. The slight positive deviation in the $[N^+]/[N]$ ratios during the deprotonation cycle may have resulted from structure alteration of the polymer due to the formation of C–Cl species.

Protonation of EM base powder with volatile HCl, followed by drying under reduced pressure, can result in the substantial removal of the protonic acid dopant in the surface region. Further removal of the dopant can readily occur for samples exposed to the ultra-high-vacuum environment during surface analyses by X.p.s. As a result, the protonation levels and the overall [Cl]/[N] ratios of the EM–HCl complexes, as revealed by X.p.s., are usually below the original levels. This limitation of the X.p.s. technique in the study of charge transfer interaction between EM base and the volatile dopant is reflected by the X.p.s. [Cl]/[N] ratios being below 0.5 in *Figure 1*. Despite the substantially reduced observable protonic acid loadings, the hysteresis effect in the intrinsic oxidation states and protonation levels of the polymer during the protonation–deprotonation cycle is clearly discernible. The reduction in the intrinsic oxidation state of the polymer, as indicated by the increase in the proportion of amine nitrogens to well above 50%, at high HCl loading must be associated with the increasing addition of HCl to the polymer. This conclusion is also consistent with the presence of a high proportion of the covalently bonded chlorine (–Cl) species at high HCl loading. Earlier infra-red absorption data of Tang *et al.*[19] and the X.p.s. results on model compounds[20] have also suggested the addition of HCl to the quinonoid units at high HCl concentration and a subsequent decrease in quinonoid/benzenoid ratio. During the deprotonation cycle, the proportion of covalently bonded Cl species remains at a high level until a substantial degree of deprotonation has occurred. As a result, the intrinsic oxidation state of the polymer persists at relatively low level, as indicated by the high amine contents (>50%), during the deprotonation cycle. The relationship between the proportion of covalently bonded Cl species and the amount of amine nitrogens is also illustrated in *Figure 2*. The removal of some covalently bonded Cl species at large extents of deprotonation is consistent with the dehalogenation process observed in poly(chloroaniline)s during the protonation–deprotonation cycles[21].

The hysteresis effect in the intrinsic oxidation states and protonation levels of the polymer is absent in the protonation–deprotonation cycle involving H_2SO_4 as the protonic acid. As there is no direct (covalent) addition of H_2SO_4 to the polymer, the proportion of amine nitrogens remains in the order of about 50% throughout most of the protonic acid loading levels, regardless of whether the polymer is undergoing protonation or deprotonation. *Figure 3* summarizes the changes in intrinsic oxidation states and protonation levels of PAN during a typical protonation–deprotonation cycle involving H_2SO_4. The good agreement between the [S]/[N] and $[N^+]/[N]$ ratios at all protonic acid loadings readily suggests that the protonic acid is incorporated in the form of monovalent anion, or HSO_4^-.

We wish to emphasize that the protonation–deprotonation hysteresis observed in the present work differs from that in proton uptake resulting from Donnan salt effect[5,22]. The apparent hysteresis reported in the earlier studies of the protonation–deprotonation cycle indicated that, at a given pH of the solution on the deprotonation leg of the cycle, the polymer retained more protons than at the same pH on the protonation leg. It has been proposed that the hysteresis arises from the difference in the composition of the solution in contact with the polymer at a given pH in both legs. Since the deprotonation was accomplished by NaOH,

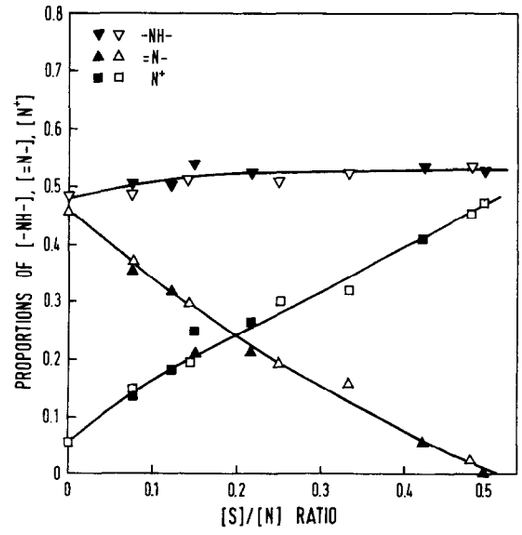

Figure 3 Changes in the intrinsic oxidation states and protonation levels of EM base powders during the protonation–deprotonation cycle involving H_2SO_4: closed symbols, deprotonation; open symbols, protonation

the solution would contain NaCl and hence be of a higher ionic strength than the corresponding protonation solution, which did not contain NaCl. The present work involves the hysteresis effect in the intrinsic oxidation state ([=N–] and [–NH–] content) and protonation level ($[N^+]/[N]$ ratio) of the polymer as a function of protonic acid loadings of the samples, and not as a function of solution pH values. Furthermore, the hysteresis effect involving HCl as the protonic acid reported in the present work is best attributed to the secondary interactions, such as covalent addition, between the acid and the polymer, as such an effect is not observed in the protonation–deprotonation cycle involving H_2SO_4.

A hysteresis of different nature exists in the protonation–deprotonation cycle involving EM films cast from *N*-methylpyrrolidinone (NMP) solution. *Figure 4a* shows the N 1s core-level spectrum for an as-cast EM film from NMP solution. *Figure 4b* shows the corresponding core-level spectrum of the film after having been protonated in 0.05 M HCl (pH ~ 1.3) for 1 h, followed by deprotonation in excess 0.5 M NaOH for 1 h. Thus, the protonation–deprotonation cycle has resulted in an increase in the intrinsic oxidation state of EM to that of the 75% intrinsically oxidized nigraniline state. Similar increase in the intrinsic oxidation state of EM films is observed for protonation–deprotonation cycles involving other protonic acids, such as 1 M HCl, 1 M H_2SO_4 and 2 M $HClO_4$. This increase in the intrinsic oxidation state after one cycle of acid–base treatment, however, is not observed in EM powders. The difference in behaviour between EM film and powder towards protonation–deprotonation can be attributed to the hindrance to water diffusion and the reduced hydrolysis reaction[7,14], which can convert imine to amine units, in the dense EM film[23] cast from NMP solution. This conclusion is consistent with the fact that the hysteresis (i.e. the increase in intrinsic oxidation state) is not observed for EM films with prolonged (>72 h) exposure to the aqueous acid medium during the protonation–deprotonation cycle. A recent scanning tunnelling microscope and atomic force microscopy study of EM film cast from NMP has revealed featureless and dense surface nanostructure before and after protonation[23]. On the other hand, each particle of EM powder is an aggregate of many small granules[24], and thus contains a large effective surface area for interaction with the environment.

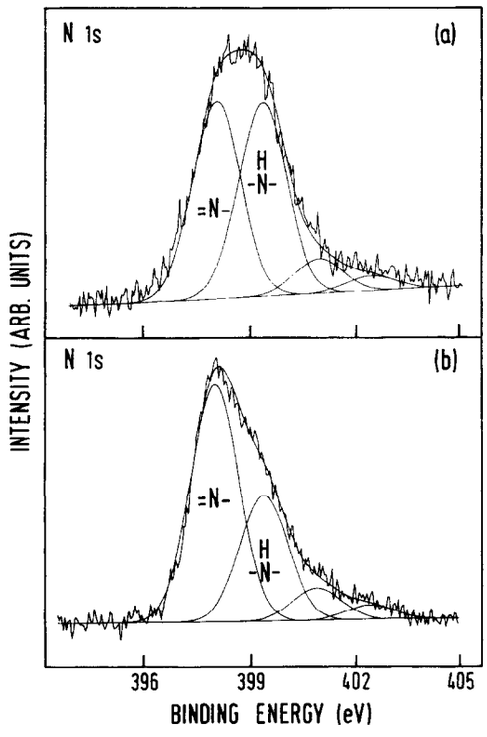

Figure 4 N 1s core-level spectra for an EM base film (a) before and (b) after one cycle of acid–base treatment in 0.05 M HCl and 0.5 M NaOH

It seems appropriate to conclude that, in the absence of hydrolysis reaction, the intrinsic oxidation state of EM base films can be substantially increased after a simple acid–base treatment. This increase in intrinsic oxidation state, however, cannot be easily observed in EM base powders for protonation–deprotonation carried out in aqueous media, owing to the loose morphology and the large effective surface area for hydrolysis associated with the powder samples. In fact, the nigraniline and the pernigraniline powders are obtained only via the oxidation of EM powders by *m*-chloroperoxybenzoic acid in a non-aqueous medium[25], or via the oxidation of leucoemeraldine powders by iodine in acetonitrile solution[15]. It should be noted that the as-cast EM film always contain a trace amount of NMP even after exhaustive pumping under reduced pressure, as NMP is a very non-volatile H-bonding plasticizer. Nevertheless, it can be completely removed during the first cycle of acid–base treatment. Finally, the possibility of oxidation of the as-cast film by the residual NMP can probably be ruled out under the present experimental conditions. Earlier studies[26] of EM and LM base in NMP solutions indicate that the former is stable in this solvent and only the latter undergoes oxidation of the amine units to imine units in the presence of dissolved oxygen. As the oxidation state of the LM polymer approaches that of EM, degradation of the polymer backbone occurs. Furthermore, in the presence of ultra-violet/visible illumination, EM base undergoes reductive degradation in NMP solution.

CONCLUSION

A hysteresis effect in intrinsic oxidation states and protonation levels of EM base powders during a protonation–deprotonation cycle was observed when HCl, but not H_2SO_4, was used as the protonic acid. The hysteresis effect arises in part from the addition of the protonic acid to the polymer. Another hysteresis effect, which involves a large increase in intrinsic oxidation state after one cycle of aqueous acid–base treatment, was observed in EM films cast from NMP, but not in EM powders. The hysteresis has been attributed to the reduced hydrolysis effect associated with the dense morphology of EM film cast from NMP.

REFERENCES

1 MacDiarmid, A. G., Chiang, J. C., Richter, A. F. and Epstein, A. J. *Synth. Met.* 1987, **18**, 285

2 Ray, A., Asturias, G. E., Kershner, D. L., Richter, A. F., MacDiarmid, A. G. and Epstein, A. J. *Synth. Met.* 1989, **29**, E141

3 Green, A. G. and Woodhead, A. E. *J. Chem. Soc.* 1910, 1117
4 Green, A. G. and Woodhead, A. E. *J. Chem. Soc.* 1910, 2388
5 Nechtschein, M., Genoud, F., Menardo, C., Mizoquchi, K., Travers, J. P. and Villeret, B. *Synth. Met.* 1989, **29**, E211
6 Neoh, K. G., Kang, E. T., Khor, S. H. and Tan, K. L. *Polym. Degrad. Stab.* 1990, **27**, 107
7 Angelopoulos, M., Asturias, G. E., Ermer, S. P., Ray, A., Scherr, E. M., MacDiarmid, A. G., Akhtar, M., Kiss, Z. and Epstein, A. J. *Mol. Cryst. Liq. Cryst.* 1988, **160**, 151
8 Cao, Y., Smith, P. and Heeger, A. J. *Synth. Met.* 1989, **31**, 263
9 Cao, Y., Smith, P. and Heeger, A. J. *Synth. Met.* 1992, **48**, 91
10 Beyer, G. and Steckenbiegler, G. *Synth. Met.* 1993, **60**, 169
11 Tan, K. L., Tan, B. T. G., Kang, E. T. and Neoh, K. G. *J. Chem. Phys.* 1991, **94**, 5382
12 Kang, E. T., Neoh, K. G. and Tan, K. L. *Surf. Interf. Anal.* 1993, **20**, 833
13 Joo, J., Oblakowski, Z., Du, G., Pouget, J. P., Oh, E. J., Weisinger, J. M., Min, Y., MacDiarmid, A. G. and Epstein, A. J. *Phys. Rev.* (*B*) 1994, **49**, 2977
14 Kang, E. T., Neoh, K. G., Woo, Y. L., Tan, K. L., Huan, C. H. A. and Wee, A. T. S. *Synth. Met.* 1993, **53**, 333
15 Kang, E. T., Neoh, K. G. and Tan, K. L. *Adv. Polym. Sci.* 1993, **106**, 135
16 Muilenberg, G. E. (Ed.) 'Handbook of X-ray Photoelectron Spectroscopy', Perkin-Elmer, Eden Prairie, MN, 1977, p. 58
17 Mirrezaei, S. R., Munro, H. S. and Parker, D. *Synth. Met.* 1988, **26**, 169
18 Dannetun, P., Lazzaroni, R., Salaneck, W. R., Scherr, E., Sun, Y. and MacDiarmid, A. G. *Synth. Met.* 1991, **41–43**, 645
19 Tang, J., Jing, X., Wang, B. and Wang, F. *Synth. Met.* 1988, **24**, 231
20 Hagiwara, T., Demura, T. and Iwata, K. *Synth. Met.* 1987, **18**, 317
21 Kang, E. T., Neoh, K. G. and Tan, K. L. *Eur. Polym. J.* 1994, **30**, 529
22 Chartier, P., Mattes, B. and Reiss, H. *J. Phys. Chem.* 1992, **96**, 3556
23 Porter, K. L., Caple, K. and Caple, G. *Synth. Met.* 1993, **60**, 211
24 Chen, S. A. and Lee, H. T. *Macromolecules* 1993, **26**, 3254
25 MacDiarmid, A. G., Manohar, S. K., Masters, J. G., Sun, Y., Weiss, H. and Epstein, A. J. *Synth. Met.* 1991, **41–43**, 621
26 Neoh, K. G., Kang, E. T. and Tan, K. L. *Polymer* 1992, **33**, 2292